

Shallow donor wavefunctions and donor-pair exchange in silicon: *Ab initio* theory and floating-phase Heitler-London approach

Belita Koiller, R.B. Capaz

Instituto de Física, Universidade Federal do Rio de Janeiro, 21945, Rio de Janeiro, Brazil

Xuedong Hu

Department of Physics, University at Buffalo, the State University of New York, Buffalo, NY 14260-1500

S. Das Sarma

*Condensed Matter Theory Center, Department of Physics,
University of Maryland, College Park, MD 20742-4111*

(Dated: December 2, 2024)

Electronic and nuclear spins of shallow donors in Silicon are attractive candidates for qubits in quantum computer proposals. Shallow donor exchange gates are frequently invoked to perform two-qubit operations in such proposals. We study shallow donor electron properties in Si within the Kohn-Luttinger envelope function approach, incorporating the full Bloch states of the six band edges of Si conduction band, obtained from *ab initio* calculations within the density-functional and pseudopotential frameworks. Inter-valley interference between the conduction-band-edge states of Si leads to oscillatory behavior in the charge distribution of one-electron bound states and in the exchange coupling in two-electron states. The behavior in the donor electron charge distribution is strongly influenced by interference from the plane-wave and periodic parts of the Bloch functions. For two donors, oscillations in the exchange coupling calculated within the Heitler-London (HL) approach are due to the plane-wave parts of the Bloch functions alone, which are pinned to the impurity sites. The robustness of this result is assessed by relaxing the phase pinning to the donor sites. We introduce a more general theoretical scheme, the floating-phase HL, from which the previously reported donor exchange oscillatory behavior is qualitatively and quantitatively confirmed. The floating-phase formalism provides a “handle” on how to theoretically anticipate the occurrence of oscillatory behavior in electronic properties associated with electron bound states in more general confining potentials, such as in quantum dots.

PACS numbers: PACS numbers: 71.55.Cn, 03.67.Lx, 85.30.-z

I. INTRODUCTION

Doping in semiconductors has significant technological impact. As transistors and integrated circuits decrease in size, the physical properties of the devices are becoming sensitive to the actual configuration of impurities. A striking example is the proposal of donor-based silicon quantum computer (QC) by Kane,¹ in which the monovalent ³¹P impurities in Si are the fundamental quantum bits (qubits). This intriguing proposal has created considerable recent interest in revisiting the donor impurity problem in silicon, particularly in the Si:³¹P system.

Two-qubit operations for the donor-based Si QC architecture, which are required for a universal QC, involve precise control over electron-electron exchange^{2,3} and electron-nucleus hyperfine interactions. Such control can presumably be achieved by fabrication of donor arrays with accurate positioning and surface gates whose potential can be precisely controlled.^{4,5,6,7} However, we have shown⁸ that electron exchange in bulk silicon has spatial oscillations on the atomic scale due to the valley interference arising from the particular six-fold degeneracy of the bulk Si conduction band. These oscillations place heavy burdens on device fabrication and coherent control, because of the very high accuracy requirement

for placing each donor inside the Si unit cell, and/or for controlling the external gate voltages.

The potentially severe consequences of these problems for exchange-based Si QC architecture motivated us and other researchers to perform further theoretical studies, going beyond some of the simplifying approximations in the formalism adopted in Ref. 8, and incorporating perturbation effects due to applied strain⁹ or gate fields.¹⁰ Both these studies, performed within the standard Heitler-London (HL) formalism,¹¹ essentially reconfirm the originally reported difficulties regarding the sensitivity of the electron exchange coupling to donor positioning, indicating that these may not be completely overcome by applying uniform strain or electric fields. At this point it is clear that the extreme sensitivity of the calculated exchange coupling to donor relative position originates from interference between the plane-wave parts of the six degenerate Bloch states associated with the Si conduction-band minima. Theoretically, this effect is dictated by the HL approximation, where the phases of the Bloch states are pinned at each donor site.

Our goal here is to assess the robustness of the HL approximation for the two-electron donor-pair states. We first examine the single donor properties in more detail by including the complete Si conduction band Bloch functions. The calculated single donor electron charge

density vividly illustrates the rapidly oscillatory (and non-commensurate) nature of the donor electron properties. We then relax the phase pinning at donor sites and allow small phase shifts in the plane-wave part of the Bloch functions, which could in principle moderate, even eliminate, the oscillatory exchange behavior. Within this more general theoretical scheme, which we call the *floating-phase* HL approach, our main conclusion is that, for all practical purposes, phase shifts are energetically unfavorable for both singlet and triplet states. The previously adopted HL wavefunctions are thus found to be robust, and the oscillatory behavior obtained in Refs. 8,9,10 cannot be taken as an artifact.

In the next section we review the shallow donor problem in Si, incorporating the Si band structure details. We present *ab initio* results for the bulk Si conduction-band-edge charge densities of individual Bloch states and single donor states. In Sec. III we consider two substitutional donors in bulk Si, and introduce the floating-phase HL approximation. The two-particle ground state energy is compared with that of the standard (pinned-phase) HL states. We present results for the donor electron exchange between P donor pairs in Si in situations of practical interest, consistent with the current degree of experimental control over donor positioning^{4,5,6} for the fabrication of Si QC. We also indicate how the floating-phase scheme may be useful for different Si-based QC architectures. Concluding remarks are presented in Sec. IV. This work thus provides necessary theoretical support and pictures to anticipated experimental studies on qubit exchange coupling in a Si matrix.

II. SINGLE DONOR IN SILICON

We determine the donor electron ground state using effective mass theory. The bound donor electron Hamiltonian for an impurity at site \mathbf{R}_0 is written as

$$\mathcal{H}_0 = \mathcal{H}_{SV} + \mathcal{H}_{VO}. \quad (1)$$

The first term, \mathcal{H}_{SV} , is the so-called single-valley Kohn-Luttinger Hamiltonian,¹² which includes the single particle kinetic energy, the Si periodic potential, and the screened impurity Coulomb potential

$$V(\mathbf{r}) = -e^2/\epsilon|\mathbf{r} - \mathbf{R}_0|. \quad (2)$$

For shallow donors in Si, we use the static dielectric constant $\epsilon = 12.1$. The second term of Eq. (1), \mathcal{H}_{VO} , includes the inter-valley coupling effects due to the presence of the impurity potential.¹³

The electron eigenfunctions are written in terms of the six unperturbed Si band edge Bloch states $\phi_\mu = u_\mu(\mathbf{r})e^{i\mathbf{k}_\mu \cdot \mathbf{r}}$:

$$\psi_{\mathbf{R}_0}(\mathbf{r}) = \sum_{\mu=1}^6 \alpha_\mu F_\mu(\mathbf{r} - \mathbf{R}_0) \phi_\mu(\mathbf{r}, \mathbf{R}_0)$$

$$= \sum_{\mu=1}^6 \alpha_\mu F_\mu(\mathbf{r} - \mathbf{R}_0) u_\mu(\mathbf{r}) e^{i\mathbf{k}_\mu \cdot (\mathbf{r} - \mathbf{R}_0)}. \quad (3)$$

The phases of the plane-wave part of all band edge Bloch states are naturally pinned at \mathbf{R}_0 , and the α_μ expansion coefficients are real. In this way the charge density at the donor site [where the donor potential (2) is more attractive] is maximum, thus minimizing the energy for $\psi_{\mathbf{R}_0}(\mathbf{r})$. In Eq. (3), $F_\mu(\mathbf{r} - \mathbf{R}_0)$ are envelope functions centered at \mathbf{R}_0 , for which we adopt the anisotropic Kohn-Luttinger form (e.g., for $\mu = z$, $F_z(\mathbf{r}) = \exp\{-([x^2 + y^2]/a^2 + z^2/b^2]^{1/2}\}/\sqrt{\pi a^2 b}$). The effective Bohr radii a and b are variational parameters chosen to minimize $E_{SV} = \langle \psi_{\mathbf{R}_0} | \mathcal{H}_{SV} | \psi_{\mathbf{R}_0} \rangle$, leading to $a = 25 \text{ \AA}$, $b = 14 \text{ \AA}$ and $E_{SV} \sim -30 \text{ meV}$ when recently measured effective mass values are used in the minimization.⁸

The \mathcal{H}_{SV} ground state is six-fold degenerate. This degeneracy is lifted by the valley-orbit interactions,^{13,14} which account for intervalley scattering effects and are included here in \mathcal{H}_{VO} . These effects are briefly reviewed in Appendix A, leading to a nondegenerate (A_1 -symmetry) ground state where all $\alpha_\mu = 1/\sqrt{6}$ in (3), and a binding energy $\sim 40 \text{ meV}$, much closer to the experimentally observed value.¹⁵

The periodic part of each Bloch function is pinned to the lattice, independent of the donor site. It can be expanded over the reciprocal lattice vectors \mathbf{G} :

$$u_\mu(\mathbf{r}) = \sum_{\mathbf{G}} c_{\mathbf{G}}^\mu e^{i\mathbf{G} \cdot \mathbf{r}}. \quad (4)$$

We determine the coefficients $c_{\mathbf{G}}^\mu$ for the conduction band edge Bloch states in Eq.(4) from *ab initio* calculations within the density-functional and pseudopotential frameworks and plane-wave basis, using the ABINIT code.¹⁶ The key ingredients of this code are an efficient Fast Fourier Transform algorithm¹⁷ for the conversion of wavefunctions between real and reciprocal space, the adaptation to a fixed potential of the band-by-band conjugate gradient method,¹⁸ and a potential-based conjugate-gradient algorithm for the determination of the self-consistent potential.¹⁹ The Troullier-Martins²⁰ pseudopotentials have been generated with the FHI98PP code.²¹ We use the local-density approximation (LDA) for the exchange-correlation functional.²² The energy cutoff for the plane-wave basis is 16 Ry. We find the equilibrium lattice constant of Si at $a = 5.41 \text{ \AA}$ and the conduction-band minima at $0.844(2\pi/a)$ from Γ , in close agreement with experimental results.¹⁵ These values are used in the calculations presented below.

In Figs. 1(a) and 1(b) we present the electronic probability density $\rho_x = |\phi_x|^2$ obtained from the *single* conduction-band-edge Bloch state $\phi_x = u_x(\mathbf{r})e^{i\mathbf{k}_x \cdot \mathbf{r}}$. Visually, our results indicate that this state is predominantly formed by $|p_x\rangle$ atomic-like orbitals, although some d -character may also be present, in consistency with the higher degree of delocalization for these states as compared to the conduction band states at the Γ point.²³

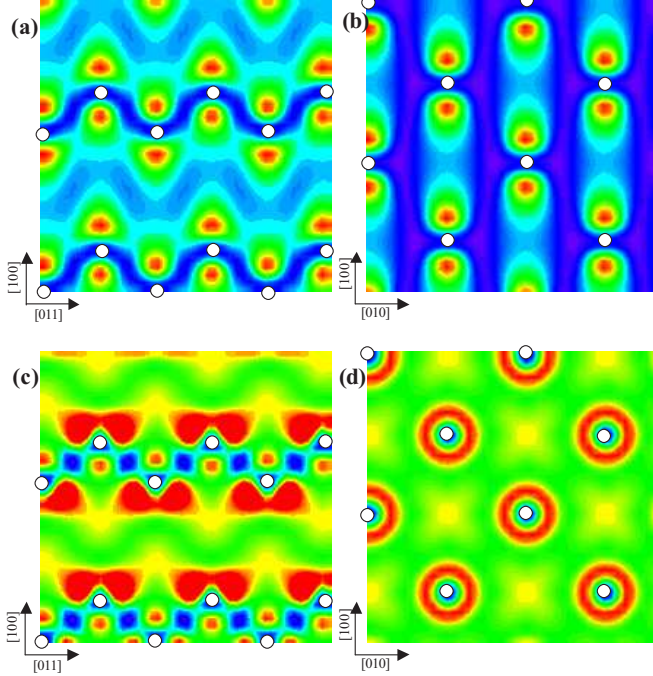


FIG. 1: (color) (a) and (b) Probability density for the single Bloch state $\rho_x = |\phi_x|^2$ in two different crystal planes. Notice the $|p_x\rangle$ atomic-like signature. (c) and (d) Total probability density for the six conduction-band minima, showing a more symmetric structure. White dots represent Si sites in the diamond structure and the color scheme runs from purple (low density) to red (high density)

Of course, as for any Bloch state, the probability density is periodic in the fcc lattice. It is also interesting to note that over 90% of the spectral weight in the plane-wave expansion of $u_x(\mathbf{r})$ in Eq.(4) comes from five reciprocal lattice vectors: $\mathbf{G} = (0, 0, 0), \frac{2\pi}{a}(-1, \pm 1, \pm 1)$. These give the five smallest values of $|\mathbf{G} + \mathbf{k}_x|$ since $k_x = 0.844\frac{2\pi}{a}(+1, 0, 0)$. This same criterion for the five most relevant coefficients $c_{\mathbf{G}}^{\mu}$ applies to each of the other five \mathbf{k}_{μ} -vectors.

In Figs. 1(c) and 1(d) we show the total charge density $\sum_{\mu=1,6} |\phi_{\mu}|^2$. Fig. 1(c) shows the characteristic antibonding signature of the conduction band state, which was also found by Richardson and Cohen²³ for the conduction-band density at the X -point in Si (thus not exactly at the band edge). The conduction band edge state of Si has been previously studied by Ivey and Mieher.²⁴ Our *ab initio* results are in good qualitative agreement with this earlier empirical pseudopotential study.

We analyze the effects of Si band structure on donor electron wavefunction within two models for the conduction band edge states $\{\phi_{\mu}\}$ of Si: (i) $\phi_{\mu, \mathbf{R}_0} = e^{i\mathbf{k}_{\mu} \cdot (\mathbf{r} - \mathbf{R}_0)}$; (ii) $\phi_{\mu, \mathbf{R}_0} = u_{\mu}(\mathbf{r}) e^{i\mathbf{k}_{\mu} \cdot (\mathbf{r} - \mathbf{R}_0)}$. Model (i) corresponds to the free-electron single-plane-wave-per-valley approximation adopted in previous studies.^{8,9,25} In model (ii) band structure contributions are fully incorporated. Regard-

ing the electron probability density plotted in Fig. 1 for model (ii), model (i) would have given completely uniform distributions, consistent with taking $u_{\mu} = 1$, i.e., $c_{\mathbf{G}}^{\mu} = \delta_{\mathbf{G}, \mathbf{R}}$ for all μ .

The effects of the conduction band states of Si on the donor wavefunctions and charge density are well established experimentally.²⁶ Particularly, the single impurity charge density is not only an interesting physical property by itself, but also foretells the oscillatory behavior in two-donor properties such as exchange. Figs. 2 (a) and (b) give the single electron charge density $|\Phi(\mathbf{r})|^2$ along a (001) crystal plane for a symmetrized state at the conduction-band edge of *bulk silicon*, $\Phi(\mathbf{r}) = (\sqrt{6})^{-1} \sum_{\mu=1}^6 \phi_{\mu, \mathbf{R}_0}(\mathbf{r})$, within models (i) and (ii) respectively. Frame (a) shows that interference from the six plane-wave states included in model (i) leads to a periodic charge pattern consistent with a simple-cubic lattice of lattice parameter $2\pi/k_{\mu} \sim 1.18a$, with a periodicity which is clearly different (and incommensurate) from the atomic positions in the lattice, since $|\mathbf{k}_{\mu}|$ is incommensurate with the reciprocal lattice. Of course a different interference pattern would result if the plane waves were not *all* pinned at site \mathbf{R}_0 . Results for model (ii) given in (b) show that additional interference from the Bloch functions $u_{\mu}(\mathbf{r})$, which are periodic in the fcc lattice, further reduce the periodicity of the charge density.

Figures 2(c) and 2(d) give the charge density $|\psi_{\mathbf{R}_0}(\mathbf{r})|^2$ for the donor state in Eq. (3), within models (i) and (ii) respectively. The impurity site \mathbf{R}_0 , corresponding to the higher charge density, is at the center of each frame. It is interesting (and somewhat counterintuitive) that, except for this central site, regions of high charge concentration and atomic sites do not necessarily coincide, because the charge distribution periodicity imposed by the plane-wave part of the Bloch functions is $2\pi/k_{\mu}$, incommensurate with the lattice period a .

III. DONOR PAIR

A. Exchange coupling within the Heitler-London approach

Within the HL approximation, the lowest energy singlet and triplet wavefunctions for two electrons bound to a donor pair at sites \mathbf{R}_A and \mathbf{R}_B are written as properly symmetrized combinations of $\psi_{\mathbf{R}_A}$ and $\psi_{\mathbf{R}_B}$, which are in turn defined in Eq. (3)

$$\Psi_t^s(\mathbf{r}_1, \mathbf{r}_2) = \frac{1}{\sqrt{2(1 \pm S^2)}} [\psi_{\mathbf{R}_A}(\mathbf{r}_1)\psi_{\mathbf{R}_B}(\mathbf{r}_2) \pm \psi_{\mathbf{R}_B}(\mathbf{r}_1)\psi_{\mathbf{R}_A}(\mathbf{r}_2)], \quad (5)$$

where S is the overlap integral and the upper (lower) sign corresponds to the singlet (triplet) state. The energy expectation values for these states are

$$E_t^s = \langle \Psi_t^s | \mathcal{H} | \Psi_t^s \rangle = 2E_0 + \frac{H_0 \pm H_1}{1 \pm S^2} \quad (6)$$

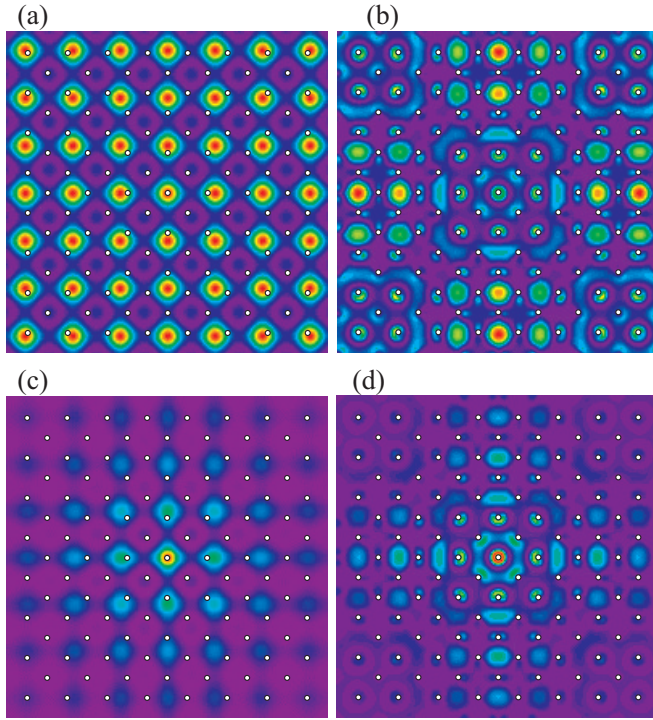


FIG. 2: (color) Frames (a) and (b) give the electron probability densities on the (001) plane of bulk Si for the bottom of the conduction band eigenstate corresponding to a symmetric combination of the six degenerate Bloch states at the conduction band edge, calculated within models (i) and (ii) respectively. Frames (c) and (d) give the corresponding probabilities for the ground state of a donor in Si within the envelope function approximation. The white dots give the in-plane atomic sites and the color scheme runs from purple (low density) to red (high density)

where E_0 is the isolated impurity binding energy and H_0 and H_1 are usually referred to as Coulomb and exchange integrals.^{9,11} The energy difference $J = E_t - E_s$ gives the exchange splitting. We have previously derived the expression for the donor electron exchange splitting in Ref.9, which we reproduce here:

$$J(\mathbf{R}) = \sum_{\mu, \nu} |\alpha_\mu|^2 |\alpha_\nu|^2 \mathcal{J}_{\mu\nu}(\mathbf{R}) \cos(\mathbf{k}_\mu - \mathbf{k}_\nu) \cdot \mathbf{R}, \quad (7)$$

where $\mathcal{J}_{\mu\nu}(\mathbf{R})$ are kernels determined by the envelopes and are slowly varying.^{8,9} Below we make a few observations before we attempt to go beyond the HL approximation.

Equation (7) does not involve any contribution from the periodic part of the Bloch functions (4) [in terms of additional oscillatory behavior in $J(\mathbf{R})$ or additional contribution to the magnitude of $J(\mathbf{R})$], which therefore may essentially be taken as $u_\mu(\mathbf{r}) = 1$. This fact has been pointed out by Wellard et al,¹⁰ and is a consequence of the pinning of the $u_\mu(\mathbf{r})$ functions to the lattice, independent of the donor site, and of their fast oscillating nature.

These authors calculated some HL integrals with \mathbf{G} different from the Γ point, which were originally neglected in Refs. 8,9,25, and confirmed numerically that all approximations adopted here (and in Ref. 9) are excellent. We therefore conclude that models (i) and (ii), though giving quite different electron probability densities as illustrated in panels (c) and (d) of Fig. 2, effectively lead to the same results for the exchange coupling within the HL approximation.

Although the exchange coupling given in Eq. (7) should be applicable to any relative position vector \mathbf{R} , including the effect of small perturbations in the donor sites into off-lattice positions,⁸ it has been pointed out by Altarelli and co-workers^{27,28} that interstitial donors in Si may acquire a deep-center character, invalidating the envelope-function treatment adopted here. We therefore focus our study on substitutional (thus shallow) donors in Si.

Figure 3 illustrates a case of practical concern involving unintentional donor displacements into nearest-neighbor sites, when donor pairs belong to different fcc sublattices.²⁹ The open squares in Fig. 3(a) give $J(\mathbf{R})$ for substitutional donors along the [100] axis, while the open triangles illustrate the different-sublattice positioning situation, namely $\mathbf{R} = \mathbf{R}_0 + \vec{\delta}_{NN}$ with \mathbf{R}_0 along the [100] axis and $\vec{\delta}_{NN}$ ranging over the four nearest-neighbors of each \mathbf{R}_0 ($d_{NN} = |\vec{\delta}_{NN}| = a\sqrt{3}/4 \sim 2.34 \text{ \AA}$). The lower panel of the figure presents the same data on a logarithmic scale, showing that nearest-neighbor displacements lead to an exchange coupling reduction by one order of magnitude when compared to $J(\mathbf{R}_0)$.

Our previous studies⁹ show that the extreme sensitivity of $J(\mathbf{R})$ to interdonor positioning is eliminated for on-lattice substitutional impurities in uniaxially strained Si (e.g. along the z axis) commensurately grown over $\text{Si}_{1-x}\text{Ge}_x$ alloys *if* \mathbf{R} remains parallel to the interface x - y plane. The strain is accommodated in the Si layer by increasing the bond-length components parallel to the interface and decreasing those along z , breaking the cubic symmetry of the lattice and lowering the six-fold degeneracy of the conduction band minimum to two-fold. In this case, the valley populations α_μ in the donor electron ground state wave function (3) are determined from a scalar valley strain parameter χ , which quantifies the amount of strain. Figure 3(b) gives $J(\mathbf{R})$ in uniaxially strained (along z direction) Si for $\chi = -20$ for the same relative positioning of the donor pairs as in Fig. 3(a). Notice that the exchange coupling is enhanced by about a factor of 2 with respect to the relaxed Si host, but the order-of-magnitude reduction in J caused by displacements of amplitude d_{NN} into nearest-neighbor sites still persists as $\vec{\delta}_{NN}$ is not parallel to the x - y plane.

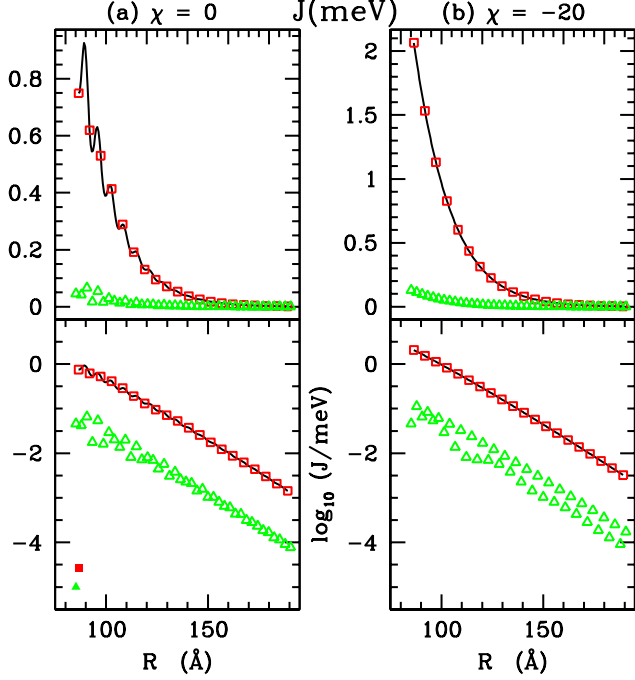


FIG. 3: Calculated exchange coupling for a donor pair versus interdonor distance in (a) unstrained and (b) uniaxially strained (along z) Si. The open squares correspond to substitutional donors placed exactly along the [100] axis, the lines give the calculated values for continuously varied interdonor distance along this axis, assuming the envelopes do not change. The open triangles give the exchange for a substitutional pair *almost* along [100], but with one of the donors displaced by $d_{NN} \sim 2.3 \text{ \AA}$ into a nearest-neighbor site. The lower frames give the same data in a logarithmic scale. Examples of corrections obtained when the floating-phase HL approach is adopted are given by the filled symbols on the lower left frame, where the data points give the log of the absolute value of the correction in J (see text).

B. Floating-phase Heitler-London approach

1. Formalism

In Refs. 8 and 9, as in the standard HL formalism presented above, it is implicitly assumed that the phases $e^{-i\mathbf{k}_\mu \cdot \mathbf{R}_0}$ in Eq. (3) remain pinned to the respective donor sites $\mathbf{R}_0 = \mathbf{R}_A$ and \mathbf{R}_B , as we adopt single donor wavefunctions to build the two-electron wavefunction. Although phase pinning to the donor substitutional site is required for the ground state of an isolated donor (A_1 symmetry) in order to minimize single electron energy, this is not the case for the lower-symmetry problem of the donor pair. In order to minimize the energy of the two-donor system, here we allow the phases to shift by an amount $\delta\mathbf{R}$ along the direction of the interdonor vector $\mathbf{R} = \mathbf{R}_B - \mathbf{R}_A$, so that the single-particle wavefunctions

in Eq. (5) become

$$\psi_{\mathbf{R}_A}(\mathbf{r}) = \frac{1}{\sqrt{6}} \sum_{\mu=1}^6 F_\mu(\mathbf{r} - \mathbf{R}_A) u_\mu(\mathbf{r}) e^{i\mathbf{k}_\mu \cdot (\mathbf{r} - \mathbf{R}_A + \delta\mathbf{R})} \quad (8)$$

and

$$\psi_{\mathbf{R}_B}(\mathbf{r}) = \frac{1}{\sqrt{6}} \sum_{\mu=1}^6 F_\mu(\mathbf{r} - \mathbf{R}_B) u_\mu(\mathbf{r}) e^{i\mathbf{k}_\mu \cdot (\mathbf{r} - \mathbf{R}_B - \delta\mathbf{R})}. \quad (9)$$

All terms appearing in Eq. (6) are now functions of $\delta\mathbf{R}$, which we take as a variational parameter here, chosen independently as $\delta\mathbf{R}_s$ and $\delta\mathbf{R}_t$ to minimize E_s and E_t (since singlet and triplet states are orthogonalized through the spin part of the wavefunction). A similar *ansatz*, the so-called floating functions approach, was suggested by Hurley³⁰ as an improvement over HL for the H_2 molecule, with the atomic orbitals symmetrically shifted towards each other. When the amplitude of the shift is taken as a variational parameter, energy reduction thus obtained leads to a significantly better agreement with experiment for the hydrogen molecule total energy.³⁰ Since the phases in Eq.(3) are responsible for the oscillatory behavior of the exchange coupling between donor electrons in Si, this more general variational treatment might lead to changes in the previously reported^{8,9,10} behavior of the two-donor exchange splitting $J = E_t - E_s$.

2. One- and two-center contributions

Adopting the floating-phase forms given in Eqs. (8) and (9) in the HL expression (5) leads to the following expression for the expectation value of the energy in Eq. (6) for the singlet and triplet states:

$$E_t^s(\mathbf{R}, \delta\mathbf{R}) = E_t^s(\mathbf{R}, 0) + \Delta_0(\delta\mathbf{R}) + \Delta_t^s(\mathbf{R}, \delta\mathbf{R}), \quad (10)$$

where $E_t^s(\mathbf{R}, 0)$ is the pinned-phase result from the regular HL calculation. The first correction term, $\Delta_0(\delta\mathbf{R})$, is the energy shift due to the single-particle single-center contributions, derived in Appendix B, and $\Delta_t^s(\mathbf{R}, \delta\mathbf{R})$ are the singlet and triplet state corrections coming from the two-center contributions H_0 , H_1 and S . The latter are integrals involving the electronic wavefunctions (8) and (9), and are calculated here as described in Ref. 9, with the proper phase shifts included in the plane-wave part of the Bloch functions.

In Fig. 4 we give the calculated values of the individual corrections $\Delta_0(\delta\mathbf{R})$ and $\Delta_t^s(\mathbf{R}, \delta\mathbf{R})$ for a geometry where the impurities are 16 lattice constants apart ($\sim 87 \text{ \AA}$), with \mathbf{R} along the [100] crystal direction. The energy correction Δ_0 raises sharply for nonzero δR , and is of course independent of the relative position vector \mathbf{R} , while the energy variations Δ_t^s oscillate and decrease with increasing relative distance R , and may be positive or negative according to δR (for $\delta R \approx 0$ in the case illustrated in

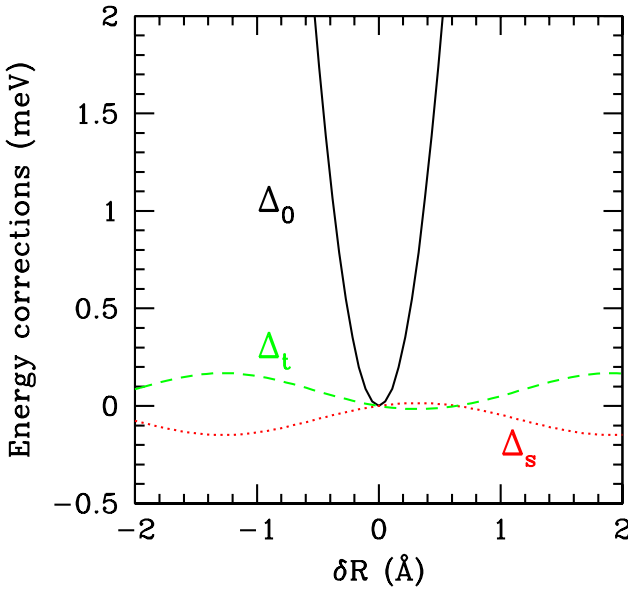


FIG. 4: Calculated corrections to the total energy for a P donor pair in Si. The donors are 87 Å apart, along the [100] direction. The parameter δR is the amplitude of the individual phase shifts from the donor sites, $\pm \delta \mathbf{R}$, along the interdonor line. The solid line gives Δ_0 , the single-center contribution, while the dotted (dashed) line gives Δ_s (Δ_t), the two-center singlet and triplet contributions, respectively.

Fig. 4, Δ_s decreases for negative shifts δR , while Δ_t decreases for positive shifts. Since Δ_0 is always positive [see Appendix B], independent of R and very sensitive to $\delta \mathbf{R}$, we conclude that the effect of phase shifts aiming at minimizing two-donor energy is negligible and may be safely ignored for $R \gg a, b$, where a and b are the donor effective Bohr radii. For example, minimization of the total energy in Eq. (10) for the particular geometry considered in Fig. 4 leads to $\delta R_s = -7$ mÅ, with the singlet energy decrease of 270 neV, and $\delta R_t = +7$ mÅ, with the triplet energy decrease of 6 neV. This results in an increase in J by (264) neV, given by the solid square in the lower left hand side frame of Fig. 3. The floating phases variational scheme leads to a reduction in both singlet and triplet states energy, therefore the net variation in J is positive (negative) if the triplet energy reduction is smaller (larger) than the singlet. The solid triangle in Fig. 3 corresponds to a case of negative variation, obtained when one of the donors in the above geometry is displaced into a nearest-neighbor site. Note that the corrections are more than three orders of magnitude smaller than the calculated J assuming $\delta R_s = \delta R_t = 0$. In other words, for all practical purposes the fixed-phase standard HL approximation is entirely adequate for the range of interdonor distances of interest for QC applications.

This conclusion is not in contradiction with Hurley's result for the hydrogen molecule,³⁰ where significant energy reduction is obtained around the equilibrium nuclear separation, $R \sim 1.5a_0$ ($a_0 = 0.53$ Å is the free hydrogen

atom Bohr radius). For R of the order of the Bohr radius, Δ_s becomes comparable to Δ_0 , resulting in an improved variational estimate for the ground state energy of the H₂ molecule when small shifts are allowed in the single-particle hydrogenic orbitals.

Since the current calculation has taken into account the full bandstructure of the host Si material, and modifying the standard HL approximation has proved to have minimal effect on the results, further improvement in a perfect crystal environment (that is, relaxed bulk Si) can only be achieved by including the higher energy orbitals.^{3,31} However, we do not anticipate significant moderation of the fast oscillatory behavior of exchange coupling as all the orbitals share the same conduction band valleys, though quantitative shifts might be expected in a larger scale molecular orbital calculation. In the present study, we keep the two donors relatively far apart so that the HL approximation is applicable. This is also the situation of interest to practical QC fabrication considerations (which requires the donors to be at least 100 Å apart).

Another improvement over our current calculation may come from including the effect of lattice distortions. The Coulomb interaction between the additional protons on the lattice sites and the two electrons for the donor pair creates a strain field on the underlying crystal lattice. Such a field affects the electronic structure in the same way as the uniaxial strain discussed above, though it is along the inter-donor axis. Since the inter-donor separation in the present situation is much larger than the effective Bohr radius (~ 30 Å), the inter-donor interaction is strongly screened, therefore lowering the strength of the strain. Furthermore, if a uniaxial strain is already applied along the z direction, so that the donor ground state only consists of the z and $-z$ valleys,⁹ the additional strain due to the presence of another donor (e.g. along x direction) will not further reduce the number of valleys involved—the nondegenerate ground state will still consist of an equally weighted superposition of these two valleys (instead of just one of them), so that oscillations in exchange due to valley interference cannot be removed.⁹ Nevertheless, a quantitative analysis is needed to assess the significance of this effect.

3. Coupled quantum dots

Shallow donors in semiconductors may be viewed as the simplest, naturally occurring quantum dot. Compared to the gated quantum dots, a relevant difference is the presence of a well defined and sharp pinning center at the substitutional donor site. Previous proposals of quantum dots as quantum gates in a Si or Ge matrix^{32,33} were based on estimates for the exchange coupling within an *empty envelope function* description. It is clear that, for these materials, the plane-wave parts of the Bloch functions may also have an important effect in the exchange coupling.

The floating-phase HL approach should be applicable

to coupled quantum dots, leading to an expression equivalent to Eq. (10). The absence of a sharp pinning center associated with each quantum dot implies that Δ_0 is not as sensitive to the phase shifts in a floating-phase variational scheme as obtained here for the donor case. It is possible that variations in the two-center contributions Δ_i^s dominate energetically and determine the singlet and tripled ground state energies, whose difference should give a reliable estimate for J .

Of course the valley-orbit effects described by \mathcal{H}_{VO} in Appendix A, which are quantitatively well established for P donors in Si, would have to be estimated for the quantum dot confining potential, including other perturbations which break the translational symmetry of the host potential, such as the presence of nearby interfaces and strain.⁹ As in the present case, \mathcal{H}_{VO} should lift the six-fold degeneracy of the isolated quantum dot ground state. An investigation of valley-orbit effects in Si quantum wells was performed recently by Boykin *et al.*³⁴

A similar scheme may also be useful for spin cluster qubits³⁵ embedded in Si or Ge, where exchange gates are also invoked for inter-cluster interactions. Demonstration that the exchange oscillatory behavior is circumvented for spin clusters would further require the formalism to be generalized to include multielectron states^{36,37} in each cluster, as was explored in Ref. 38.

IV. CONCLUDING REMARKS

We have included and assessed full band structure effects in the single donor wavefunctions and charge distributions in Si. We find interesting oscillatory patterns resulting from interference between the different plane wave components of the Bloch functions. Regarding the well-separated donor pair problem, we introduced a generalized scheme—the floating-phase HL approach, which reconfirmed the reliability of standard HL for this range of donor separations.

One perceived advantage¹ of Si-based spin quantum computation (over, for example, the corresponding GaAs quantum dot based quantum computation) is the universal nature of each qubit in Si, i.e. the fact that the P donor electronic state in Si is always exactly the same, making each qubit identical (without any need for additional characterization of individual qubits which will surely be needed for GaAs quantum dot quantum computers since electrostatically confined electronic spin states in GaAs quantum dots would obviously have a fair amount of qubit to qubit variations). Our finding of exchange oscillations in Si donor states demonstrates that this perceived advantage of Si comes with a price, where the exchange coupling between qubits may vary depending on the precise positioning of the P atoms within the Si unit cells. In spite of this problem, the QC scheme with donors in Si still has its appeal in terms of uniform qubits. Obviously characterization of the exchange coupling in Si becomes necessary in view of the oscillatory

exchange. We have discussed elsewhere³⁹ how some precise local information about donor state exchange coupling in Si can be obtained by using the powerful tool of the micro-Raman scattering spectroscopy. In addition, various band engineering procedures,⁹ using strain effects and/or Si-Ge quantum dots, could be utilized to reduce the exchange oscillation effects, although its complete elimination may not be easy.

From the perspective of current QC fabrication efforts, ~ 1 nm accuracy in single P atom positioning has been recently demonstrated,⁵ representing a major step towards the goal of obtaining a regular donor array embedded in Si. As expected,⁵ this degree of control is entirely compatible with the operations involving the so-called A-gates⁴⁰ in the Kane qubit architecture.¹ On the other hand, the present calculations have confirmed that deviations in the relative positioning of donor pairs with respect to perfectly aligned substitutional sites along [100] lead to order-of-magnitude changes in the exchange coupling. Severe limitations in controlling J would come from “hops” into different fcc sublattices, in particular among nearest-neighbor substitutional sites. Therefore, precisely controlling exchange gates in Si remains an open challenge.

Acknowledgments

We thank Alexei Kaminski for valuable help with the preparation of the manuscript. This work was partially supported by ARDA and LPS at the University of Maryland, by ARDA and ARO at the University at Buffalo, and by Brazilian agencies CNPq, FUJB, FAPERJ, PRONEX-MCT and Instituto do Milênio de Nanociências-CNPq.

APPENDIX A

Valley-orbit effects are conveniently represented by two types of intervalley couplings $\mathcal{H}_{VO_{\mu,\nu}}$: For valleys at perpendicular directions (e.g., $\mu = x, \nu = z$) we take the coupling $\mathcal{H}_{VO_{x,z}} = -\Delta_C$ while for those in opposite directions (e.g., $\mu = z, \nu = -z$), $\mathcal{H}_{VO_{z,-z}} = -\Delta_C(1 + \delta)$. Of course $\mathcal{H}_{VO_{\mu,\mu}} = 0$. Taking $\Delta_C = 2.16$ meV and $\delta = -0.3$ correctly reproduces⁹ the ordering and relative splittings of the lowest energy states manifold for P donors in Si: A ground state of A_1 symmetry, followed by a triplet of T_1 symmetry and by a doublet of E symmetry. The nondegenerate A_1 ground state corresponds to all $\alpha_\mu = 1/\sqrt{6}$ in (3), and its binding energy is $E_0 = \langle \psi_{\mathbf{R}_0} | \mathcal{H}_0 | \psi_{\mathbf{R}_0} \rangle = E_{SV} - (5 + \delta)\Delta_C \sim -40$ meV, to be compared to the experimental value of -45 meV. More sophisticated approaches such as multi-valley effective mass (MVEM) theories have been developed for impurities in Si.¹⁴ We do not adopt such an approach in order to maintain a simple and clear physical picture, as approaches like MVEM mostly provide better estimates

for the binding energy, but do not seriously alter the valley interference features.

APPENDIX B

The term $2E_0$ on the right hand side of Eq. (6) gives the single-particle single-center contributions from both (isolated) impurities, which should be taken here as $E_A + E_B = 2E_A$. For the present model Hamiltonian, within the floating phase HL approximation, we get

$$E_A(\delta\mathbf{R}) = \langle \psi_{\mathbf{R}_A} | \mathcal{H}_A | \psi_{\mathbf{R}_A} \rangle$$

$$= E_{SV} - \frac{\Delta_C}{3} [2(\cos \phi_x + \cos \phi_y + \cos \phi_z)^2 + \delta(\cos 2\phi_x + \cos 2\phi_y + \cos 2\phi_z) - 3], \quad (B1)$$

where $\phi_\mu = -\phi_{-\mu} = \mathbf{k}_\mu \cdot \delta\mathbf{R}$. The parameters Δ_C and δ are defined in Appendix A, where their numerical values are also given. As expected, for $\delta\mathbf{R} = 0$ the above expression leads to $E_A(0) = E_0 = E_{SV} - (5 + \delta)\Delta_C$, while $\delta\mathbf{R} \neq 0$ leads to $E_A(\delta\mathbf{R}) = E_0 + \frac{\Delta_0}{2} \geq E_0$. The correction Δ_0 is positive definite by construction, since the one-particle functions in standard HL ($\delta\mathbf{R} = 0$) are taken as the ground-state wavefunction of the isolated impurity problem.

¹ B. Kane, *Nature* **393**, 133 (1998).
² C. Herring and M. Flicker, *Phys. Rev.* **134**, A362 (1964).
³ X. Hu and S. Das Sarma, *Phys. Rev. A* **61**, 062301 (2000).
⁴ J. L. O'Brien, S. R. Schofield, M. Y. Simmons, R. G. Clark, A. S. Dzurak, N. J. Curson, B. E. Kane, N. S. McAlpine, M. E. Hawley, and G. W. Brown, *Phys. Rev. B* **64**, 161401 (2001).
⁵ S. R. Schofield, N. J. Curson, M. Y. Simmons, F. J. Rueß, T. Hallam, L. Oberbeck, and R. G. Clark, *Phys. Rev. Lett.* **91**, 136104 (2003).
⁶ T. M. Buehler, R. P. McKinnon, N. E. Lumpkin, R. Brenner, D. J. Reilly, L. D. Macks, A. R. Hamilton, A. S. Dzurak, and R. G. Clark, *Nanotechnology* **13**, 686 (2002).
⁷ T. Schenkel, A. Persaud, S. J. Park, J. Nilsson, J. Bokor, J. A. Liddle, R. Keller, D. H. Schneider, D. W. Cheng, and D. E. Humphries, *J. Appl. Phys.* **94**, 7017 (2003).
⁸ B. Koiller, X. Hu, and S. Das Sarma, *Phys. Rev. Lett.* **88**, 027903 (2002).
⁹ B. Koiller, X. Hu, and S. Das Sarma, *Phys. Rev. B* **66**, 115201 (2002).
¹⁰ C. J. Wellard, L. C. L. Hollenberg, F. Parisoli, L. Kettle, H.-S. Goan, J. A. L. McIntosh, and D. N. Jamieson, *arXiv:cond-mat/0309417* (2003).
¹¹ J. C. Slater, *Quantum Theory of Molecules and Solids*, vol. 1 (McGraw-Hill, New York, 1963).
¹² W. Kohn, *Solid State Physics Series*, vol. 5 (Academic Press, 1957), edited by F. Seitz and D. Turnbull, p.257, and references therein.
¹³ A. Baldereschi, *Phys. Rev. B* **1** (1970).
¹⁴ S. T. Pantelides, *Rev. Mod. Phys.* **50** (1978).
¹⁵ O. Madelung, *Semiconductors-Basic Data* (Springer, Berlin, 1996).
¹⁶ X. Gonze, J.-M. Beuken, R. Caracas, F. Detraux, M. Fuchs, G.-M. Rignanese, L. Sindic, M. Verstraete, G. Zerah, F. Jollet, et al., *Computational Materials Science* **25** (2002), (URL <http://www.abinit.org>).
¹⁷ S. Goedecker, *SIAM J. on Scientific Computing* **18** (1997).
¹⁸ M. C. Payne, M. P. Teter, D. C. Allan, T. A. Arias, and J. D. Joannopoulos, *Rev. Mod. Phys.* **64** (1992).
¹⁹ X. Gonze, *Phys. Rev. B* **54** (1996).
²⁰ N. Troullier and J. L. Martins, *Phys. Rev. B* **43**, 1993 (1991).
²¹ M. Fuchs and M. Scheffler, *Comput. Phys. Commun.* **119**, 67 (1999).
²² D. M. Ceperley and B. J. Alder, *Phys. Rev. Lett.* **45**, 566 (1980).
²³ S. L. Richardson and M. L. Cohen, *Phys. Rev. B* **35**, 1388 (1987).
²⁴ J. L. Ivey and R. L. Mieher, *Phys. Rev. B* **11**, 822 (1974).
²⁵ K. Andres, R. N. Bhatt, P. Goalwin, T. Rice, and R. Walstedt, *Phys. Rev. B* **24**, 244 (1981).
²⁶ G. Feher, *Phys. Rev. B* **114**, 1219 (1959).
²⁷ M. Altarelli and W. L. Hsu, *Phys. Rev. Lett.* **43**, 1346 (1979).
²⁸ H. Weiler, N. Meskini, W. Hanke, and M. Altarelli, *Phys. Rev. B* **30**, 2266 (1984).
²⁹ In MBE growth of donor arrays in Si, currently available technology does not allow differentiation for donor positioning among the two sites within one dimer (which are surface-nearest-neighbor to each other) of the Si (001) surface.⁴ We believe a similar difficulty occurs for the 3D lattice nearest-neighbor sites.
³⁰ A. C. Hurley, *Proc. Roy. Soc. A* **226** (1954).
³¹ R. A. Faulkner, *Phys. Rev.* **184**, 713 (1969).
³² J. Levy, *Phys. Rev. A* **64**, 052306 (2001).
³³ M. Friesen, P. Rugheimer, D. E. Savage, M. G. Legally, D. W. van der Weide, and R. Joyst, *Phys. Rev. B* **67**, 121301 (2003).
³⁴ T. B. Boykin, G. Klimeck, M. A. Eriksson, M. Friesen, S. N. Coppersmith, P. von Allmen, F. Oyafuso, and S. Lee, *Appl. Phys. Lett.* **84** (2004).
³⁵ F. Meier, J. Levy, and D. Loss, *Phys. Rev. Lett.* **90**, 047901 (2003).
³⁶ X. Hu and S. Das Sarma, *Phys. Rev. A* **64**, 042312 (2001).
³⁷ S. Vorotjsov, E. Mucciolo, and H. Baranger, *arXiv:cond-mat/0308118* (2003), to appear in *Phys. Rev. B*.
³⁸ A. Mizel and D. Lidar, *arXiv:cond-mat/0302018* (2003).
³⁹ B. Koiller, X. Hu, H. D. Drew, and S. Das Sarma, *Phys. Rev. Lett.* **90**, 067401 (2003).
⁴⁰ A. S. Martins, R. B. Capaz, and B. Koiller, *arXiv:cond-mat/0308575* (2003), to appear in *Phys. Rev. B*.